ACCP
American College of Clinical Pharmacology
Advancing Clinical Care through Pharmacology

Original Article

Population Pharmacokinetics of Oral Brepocitinib in Healthy Volunteers and Patients

Clinical Pharmacology in Drug Development
2022, 11(12) 1447–1456

DOI: 10.1002/cpdd.1163

Jim H. Hughes, Ruolun Qiu, Christopher Banfield, Martin E. Dowty, and Timothy Nicholas

Abstract

Brepocitinib is a tyrosine kinase 2 and Janus kinase 1 inhibitor in development for treatment of inflammatory autoimmune diseases. This analysis aimed to add to the pharmacokinetic knowledge of the medication, through development of a population pharmacokinetic model and identification of factors that affect drug disposition. Plasma samples from 5 clinical trials were collated, composed of healthy volunteers, patients with psoriasis and patients with alopecia areata taking oral brepocitinib. NONMEM was used to develop a population pharmacokinetic model, and patient demographics were tested as covariates. The final model was a 1-compartment model with first-order absorption. The typical values for apparent clearance and apparent volume of distribution were 18.7 L/h (78% coefficient of variation [CV]) and 136 L (60.5% CV), respectively. Absorption was rapid with an absorption constant of 3.46 h, with an absorption lag of 0.24 hours observed with the oral tablet formulation. The proportional residual error was found to be 52.7% CV in healthy volunteers and 87.5% CV in patients. High-fat meals were associated with a reduction in both the rate (69.9% lower) and extent (28.3% lower) of absorption, while Asian populations had reduced clearance (24.3% lower). Nonlinear pharmacokinetics were observed at doses of 175 mg and above, with a 35.1% higher relative bioavailability at these doses. There were insufficient data to describe this nonlinearity as a continuous relationship. This initial description of the population pharmacokinetics will act as a foundation for the model-informed drug development of brepocitinib and will facilitate future modeling of this medicine. ClinicalTrials.gov numbers NCT02310750 NCT03236493 NCT03656952 NCT02969018 NCT02974868.

Keywords

alopecia, JAK inhibitor, pharmacokinetics, psoriasis

Brepocitinib (also known as PF-06700841) is a tyrosine kinase (TYK2) and Janus kinase (JAK1) inhibitor that is selective over other human kinases and proposed for treatment of a range of inflammatory autoimmune diseases.[1] TYK2 and JAK1 are part of a group of cytoplasmic tyrosine kinases responsible for the mediation of signal transduction critical for activation, proliferation, survival, and function of leukocytes[2]. Key cytokines implicated in the pathophysiology of chronic plaque psoriasis, psoriatic arthritis, Crohn disease, dermatomyositis, and systemic lupus erythematosus such as interleukin (IL)-12 and IL-23, require TYK2 for signal transduction, while JAK1 is required for IL-6, IL-21, IL-22, interferon (IFN)-α, and IFN-γ.[3] Both kinases are also critical for regulating signal transduction pathways triggered by cytokines implicated in the pathogenesis of alopecia areata, vitiligo, chronic hand eczema, and ulcerative colitis, while also blocking the production of proinflammatory cytokines, IFNs, and IL-17 through upstream inhibition of the IL-12/T-helper 1 cell and IL-23/T-helper 17 pathways.[3–5]

Brepocitinib has been evaluated in patients with plaque psoriasis and alopecia areata and in healthy participants,[6–8] with further studies ongoing in other autoimmune diseases. The first-in-human trial (NCT02310750) explored a dose range of 1 mg through to 200 mg without reaching a maximum tolerated dose.[6] In this phase 1 study, brepocitinib demonstrated efficacy in the psoriasis cohorts as measured by Psoriasis Area and Severity Index (PASI). The mean PASI scores decreased from baseline in a dose-dependent manner during the 4-week treatment period. This decrease continued in the follow-up period for both the 30- and

Pfizer Global Research and Development, Groton, Connecticut, USA

Submitted for publication 26 April 2022; accepted 8 August 2022.

Corresponding Author:
Jim Hughes, PhD, Pfizer Research and Development, 445 Eastern Point Road, Groton CT 06340
(e-mail: Jim.hughes@pfizer.com)

100-mg daily dosing regimens. Cellular responses after treatment in patients with plaque psoriasis also showed that doses of 30 and 100 mg were sufficient to attenuate cytokines responsible for driving psoriasis.[9] While a dose-dependent increase in efficacy was observed in these patients, doses of ≤60 mg were chosen for further investigation due to uncertainty around the causality of infection-related adverse events observed at higher doses.[6]

In a subsequent phase 2a trial, patients with moderate to severe plaque psoriasis (NCT0296018) received 30 or 60 mg of brepocitinib daily or placebo for a 4-week induction period, followed by 10 mg daily, 30 mg daily, 100 mg once weekly, or placebo for an 8-week maintenance period. Greater proportions of patients achieved PASI 75 and PASI 90 and clear or almost clear Physicians Global Assessment scores at week 12 in all active treatment groups versus placebo. The greatest proportion of responders were observed in the patients taking 30 mg for the entire treatment period, suggesting that brepocitinib does not require an induction dose to produce optimum efficacy.[7]

A randomized and placebo-controlled phase 2 trial was also conducted involving patients with moderate to severe alopecia areata (NCT02974868). Brepocitinib treatment with 4-week induction of 60 mg daily followed by 20-week maintenance of 30 mg daily demonstrated efficacy compared to placebo, with improvements in Severity of Alopecia Tool scores observed after induction and further improvement after the maintenance period.[8] Brepocitinib was generally well tolerated in both phase 2 trials with all test doses, covering doses up to 60 mg daily and treatment durations up to 24 weeks.

The pharmacokinetics (PK) of brepocitinib have been characterized using noncompartmental analysis in both healthy volunteers and patients. Brepocitinib is absorbed rapidly following oral administration (median time to maximum concentration 1 hour or less) and has a half-life of approximately 3.8–7.5 hours after single doses and 4.9–10.7 hours after multiple doses. Brepocitinib exhibits linear PK at doses lower than 100 mg, with doses of 100–200 mg resulting in more than dose-proportional increases in both exposure (area under the plasma concentration–time curve from time 0 to infinity) and maximum concentration.[6] Administration of tablet formulations of brepocitinib with a high-fat meal is reported to reduce both area under the plasma concentration–time curve from time 0 to infinity and maximum concentration by ≈17.7% and 35.7%, respectively, indicating that the tablet can be taken with or without food.[6] Elimination of brepocitinib is predominantly due to cytochrome P450 (CYP)-mediated metabolism (fraction hepatically metabolized: CYP3A4/5 = 0.77, CYP1A2 = 0.14) with urinary recovery of unchanged drug being low (<16%). Brepocitinib is the major circulating drug species (47.8%) in plasma, with one major pharmacologically inactive monohydroxylated metabolite (37.1%). Brepocitinib is not highly bound to plasma proteins (fraction unbound, 0.61). No substantial difference has been observed when comparing brepocitinib exposure between healthy participants and patients with plaque psoriasis or alopecia areata given the same dose; however, steady-state exposures in six healthy Japanese adults from a Japanese PK study were observed to be approximately 50% higher than exposures seen in healthy White adults from other studies.

The objective of the present analysis is to further characterize the population PK of brepocitinib and quantify the impact of different factors on brepocitinib PK using pooled data from healthy volunteers and patients from 5 phase 1 or phase 2 studies. Population PK analyses are a key part of model-informed drug development (MIDD) aimed at expediting decision making and reducing cost and time associated with drug development.[10] As a part of MIDD, the results provided by this analysis are planned be used for determining post hoc estimates of brepocitinib exposure in patients with sparse PK sampling data, for future exposure-response analysis of efficacy and safety outcomes.

Methods

Study Data

Data used in the analysis were collated from 5 clinical trials comprising 3 phase 1 (NCT02310750, NCT03236493, NCT03656952) and 2 phase 2 (NCT02969018, NCT02974868) clinical trials. All study protocols, their amendments, and informed consent documentation for studies included in the analyses were reviewed and approved by institutional review boards, and all studies were conducted in accordance with Good Clinical Practice, the Declaration of Helsinki, and local regulations.

In clinical trial NCT02310750,[6,9] healthy participants were dosed with oral brepocitinib suspension administered as a single dose of 1, 3, 10, 30, 100, and 200 mg, as multiple doses given 10, 30, 100, and 175 mg once daily or 50 mg twice daily for 10 days or as single doses of 100 mg compared with administration of a tablet formulation taken while fasting or with a high-fat meal (800–1000 calories with 500–600 calories from fat). NCT03236493 studied healthy Japanese participants taking 100-mg oral brepocitinib tablets once daily for 10 days. In the concentration-QT study (NCT03656952), healthy participants received a single dose of 200 mg oral brepocitinib as a part of standard dosing sequences with placebo and moxifloxacin.

In the phase II trial NCT02969018,[7] patients with plaque psoriasis received a 4-week induction of oral brepocitinib tablets followed by 8 weeks of maintenance dosing, with doses different between study arms. Patients were given an induction dose of 30 or 60 mg once daily followed by 10 or 30 mg once daily, 100 mg once weekly, or placebo as maintenance. Finally, NCT02974868[8] studied the treatment of patients with alopecia areata treated with a 4-week induction of 60-mg oral brepocitinib tablets followed by 20 weeks of maintenance dosing at 30 mg.

Concentrations of brepocitinib in plasma samples were analyzed for brepocitinib concentrations using a liquid chromatography–tandem mass spectrometric method. Brepocitinib and internal standard were isolated from 50.0 μL of human plasma using a protein precipitation extraction procedure with 400 μL of acetonitrile. After vortexing, centrifugation, and dilution, the mixture was analyzed by electrospray ionization liquid chromatography–tandem mass spectrometry using the positive ionization mode. The chromatographic separation was achieved using a Kinetex HILIC Silica 2.6 μm column and gradient elution (Phenomenex, Torrance, California). Mass transitions monitored were 390.2–340.2 for brepocitinib and 395.2–345.2 for internal standard. The lower limit of quantification for this assay was 0.2 ng/mL in all studies with intra- and interassay precision being ≤6.0% and ≤4.1%, respectively. Methods for handling plasma concentrations below the limit of quantification (BLQ) were considered on the basis of the proportion of BLQ values in the final analysis data set.[11,12] A full description of sampling times, study sites, and investigators for each clinical trial are provided in the Supplemental Information.

Base Model

The model was evaluated for both 1- and 2-compartment kinetics based on previous analyses. Lag time (A_{lag}) and allometric scaling on apparent clearance (CL/F), apparent central volume (Vc/F), apparent intercompartmental clearance, and apparent peripheral volume were assessed as part of the structural model.[13] Interindividual variability (IIV) was assumed to be log-normally distributed for PK parameters (Equation 1). Suitability of additional random-effect parameters and models with and without covariance for random effects using an off-diagonal variance-covariance matrix were assessed.

$$P_i = \theta_P \cdot e^{\eta_i} \tag{1}$$

where P_i is the individual value for parameter, P, in the ith individual, θ_P is the population typical value for parameter P, and η_i is an independent random variable describing the variability in P among subjects with a mean of 0 and variance, ${\omega_P}^2$.

Table 1. Covariates Evaluated During Model Development

Parameter	Covariate
k_a, A_{lag}	Fed status, dose, formulation
CL/F	Body weight, dose, patient type, race, age, sex
Vc/F	Body weight, age, sex
F_{rel}	Fed status, dose, patient type

A_{lag}, absorption lag time; CL/F, apparent clearance; F_{rel}, relative bioavailability; k_a, absorption rate constant; Vc/F, apparent central volume of distribution.

Residual unexplained variance models were assessed using a log-transform both sides approach[14] with both proportional and combined error models tested (Equations 2 and 3).

$$\ln(DV_{ij}) = \ln\left(IPRED_{ij}\right) + \theta_{pro} \cdot \varepsilon_{ij} \tag{2}$$

$$\ln\left(DV_{ij}\right) = \ln\left(IPRED_{ij}\right) + \sqrt{\left(\theta_{pro}^2 + \frac{\theta_{add}^2}{IPRED_{ij}^2}\right)} \cdot \varepsilon_{ij} \tag{3}$$

where DV_{ij} is the observed brepocitinib concentration in subject i at observation j, $IPRED_{ij}$ is the individual predicted concentration, and ε_{ij} is a normally distributed error term with a mean of 0 and a fixed variance of 1, while θ_{pro} and θ_{add} are the proportional and additive components of the residual error, respectively.

Full Covariate Model

Once the base structural model was finalized, a full covariate model was developed using full model estimation.[15–19] All covariates of interest were simultaneously added to the final base model to assess the influence and precision of each covariate. Covariates of interest were selected a priori to explore populations of interest to determine the need for alternate dosing, while also investigating covariates observed in noncompartmental and exploratory analyses. These covariates are defined in Table 1. The effect of categorical covariates was represented as a discrete relationship (Equation 4), while the effect of continuous covariates was represented as a power function referenced to the median of the observed data (Equation 5).

$$P_i = \theta_P \cdot e^{\eta_i} \cdot PCOV$$
$$\text{for } PCOV = \begin{cases} 1 & \text{if } COV = 0 \\ 1 + \theta_{PCOV} & \text{if } COV = 1 \end{cases} \tag{4}$$

$$P_i = \theta_P \cdot e^{\eta_i} \cdot \left(\frac{COV_i}{COV_{ref}}\right)^{\theta_{cov}} \quad (5)$$

where COV is a categorical covariate with a value of 0 or 1, COV_i is the continuous covariate in the ith subject, COV_{ref} is the median value for the covariate in the observed populations, θ_{PCOV} is the estimable parameter for the effect of the categorical covariate on P when COV is equal to 1 and θ_{COV} is the estimable parameter for the effect of the continuous covariate on P.

Once the full covariate model was developed, it was evaluated using a stratified nonparametric bootstrap to control for the inflated false-positive rate associated with multiple tests.[20] Bootstrap resampling was performed 1000 times using sampling with replacement. Population parameters were estimated for each bootstrap data set, with the median and 95%CIs for each parameter calculated to assess parameter uncertainty. The resulting median and 95%CI of each covariate from nonparametric bootstrap were assessed to determine whether the covariate effect (1) was clinically important (entire CI contains clinically important values that fall outside of a 80%–125% range of the reference population), (2) was statistically significant (CI does not include the mean estimate of the reference population), or (3) had insufficient information to determine importance (CI spans across both clinically important and unimportant values).[17,19]

Final Model

Finally, the full covariate model was reduced to a final parsimonious model that could be used for simulation and development of future MIDD analyses. Model reduction was achieved using a single backwards-elimination step where all covariate effects that were classified as being both not clinically important and not statistically significant by the full model estimation process were removed.[17,19] The precision of the final model was evaluated using a stratified nonparametric bootstrap, while the predictive performance of the final model was evaluated by visual predictive check (VPC) and prediction-corrected VPC based on 1000 simulations of the index data set.[21–24] Subpopulations (by study, covariates, dosing regimen, formulation, etc) were used to stratify this summary of the predictive performance.

Software and Model Selection

The population PK model was developed using nonlinear mixed-effects methods in NONMEM version VII level 4.1 (ICON plc, North Wales, Pennsylvania).[25] Population parameter estimation used first-order conditional estimation with interaction, and individual parameters were obtained from empirical Bayes post hoc estimates. Exploratory analysis, model diagnostic plots, and postprocessing of NONMEM output was generated using the R statistical and programming language version 3.5.1 (R Foundation for Statistical Computing, Vienna, Austria)[26] with the tidyverse, mrgsolve and ggridges packages. Perl-speaks-NONMEM[27] was used for nonparametric bootstraps of the full and final models and was stratified by study to reduce the impact of heterogeneity in sampling schedules on bootstrap performance.[28]

Model selection was guided by (1) the Aikaike information criterion,[29] (2) diagnostic plots,[22] (3) plausibility of parameter estimates, (4) parameter precision (obtained by both parametric and nonparametric methods), and (5) model conditioning (obtained from eigen values).[30,31] Diagnostic plots used to assess model performance included observed concentrations versus both population and individual predictions, conditional weighted residuals[32] versus time or population predictions, distribution density, and quantile-quantile plots of both conditional weighted residuals and η values and individual predicted concentration-time profiles overlaid with observations.

Results

Study Data

The PK data used for the analysis were sampled from 379 subjects. Plasma samples taken during the maintenance dose period for patients administered a 30-mg or 60-mg daily induction dose followed by a 100-mg weekly maintenance dose were not used in the analysis due to a high proportion of missing observations (≈68% of the 511 maintenance-period plasma samples taken) causing uncertainty around the timing of brepocitinib administration in relation to the time of sampling. The plasma samples taken during induction dosing for these patients were still included for analysis. The final analysis data set consisted of 5541 brepocitinib plasma observations, with 10.8% of those observations being missing or BLQ. No data imputation or methods for handling BLQ data were performed during model development with BLQ plasma concentrations considered missing during analysis; however, a sensitivity analysis was conducted using alternate BLQ handling methods on the final model.[11,12] Summaries of the demographics for these subjects are presented in Table 2.

Base Model

Both 1-compartment and 2-compartment models were built in parallel, with key steps being mirrored between the two models. A two-compartment model was not

Table 2. Demographic and Clinical Information for Clinical Trials

Continuous	Mean (SD)	Median (Range)
Age (y)	41.9 (12.9)	42 (18–75)
Body weight (kg)	86.6 (22.0)	83 (45–204)
Creatinine clearance (mL/min)	132.7 (38.7)	124 (58–279)
Categorical	**Count**	**Percentage**
Formulation		
Tablet	313	83
Suspension	66	17
Sex		
Male	263	69
Female	116	31
Race		
White	311	82
African American	19	5
Asian	30	8
Other race	19	6
Patient status		
Healthy individual	92	24
Plaque psoriasis	210	55
Alopecia areata	77	20

SD, standard deviation.

chosen as the estimation of apparent peripheral volume was highly dependent on the initial estimates for the parameter, with final estimates lacking precision. The base model chosen for full model estimation was a one-compartment model with first-order absorption and an absorption lag for the tablet formulation. IIV was included on CL/F and Vc/F with a full variance-covariance matrix. A proportional error model was used, with separate error parameters estimated for phase 1 and phase 2 studies. The effect of allometrically scaled body weight on CL/F and Vc/F and high-fat meals on the absorption-rate constant (k_a) were included as structural covariates. A table describing key model development steps can be found in the Supplemental Information.

Full Covariate Model

The full model was developed where covariates were estimated on k_a rather than A_{lag} as this resulted in better predictions and parameter precision. Before full-model estimation, dose effect and patient effect were trialed on CL/F and relative bioavailability (F_{rel}). The most informative model had patient effect on CL/F and dose effect on F_{rel}. Allometric scaling on CL/F could not be estimated with adequate precision during full-model estimation. As a result, the allometric coefficients were fixed to literature values (70 kg reference weight, 0.75 for clearance parameters, 1.0 for volume parameters).[13] The viability of a continuous relationship for the effect of dose on F_{rel} was explored; however, the models identified in this process provided minimal improvements in both objective function value and predictive performance and were not explored further.

A graphical presentation of the results of the full covariate model estimation are shown in Figure 1. This depicts the distribution of the ratio of CL/F, F_{rel}, and k_a fixed effects for each covariate estimate compared to the reference population estimate across the 1000 bootstraps. The significance of covariates is represented by range of relative parameter values within the 5th and 95th percentiles of the bootstrap estimates (statistical significance) and the proportion of estimates that resulted in a 20% difference from the population typical parameter (clinical significance). The effect of a high-fat meal on k_a (part of the base model) was the only covariate effect that was both clinically and statistically significant. In addition to these effects, the effect of Asian race on CL/F, dose $\geq$175 mg on F_{rel}, and high-fat meal on F_{rel} were statistically significant. The effect of dose and formulation on k_a were also found to be statistically significant; however, they were not considered for the final model due to the resulting k_a estimates not being meaningfully different from the population estimate. Additional exploratory covariate analysis performed based on eta versus covariate diagnostics identified that the effect of other races (ie, Native American and Pacific Islander) on CL/F were also statistically significant but were not included in the full or final model due to the low number of subjects available with full PK profiles ($n \leq 3$).

Final Model

The final model incorporated covariates identified as significant by full model estimation, including the effect of high-fat meal on k_a and F_{rel}, the effect of Asian race on CL/F and the effect of doses $\geq$175 mg on F_{rel}. The final model parameter estimates are listed in Table 3, with the equations representing individual parameter calculations presented Equations (6)–(10). The elimination half-life of brepocitinib for the reference population (70-kg non-Asian subjects) was 5.04 hours. The final model was well conditioned with a condition number <400, and parameter estimates were estimated with sufficient precision.

Due to the low proportion of BLQ values, these concentrations were treated as missing during analysis. To test the impact of this decision on final model parameters, a sensitivity analysis was performed where censored BLQ values were included in the calculation of the objective function value by determining the likelihood of BLQ observations truly being BLQ.[11] A comparison of the final model parameters with this sensitivity analysis is included in the Supplemental Information and shows that only the IIV of CL/F had a

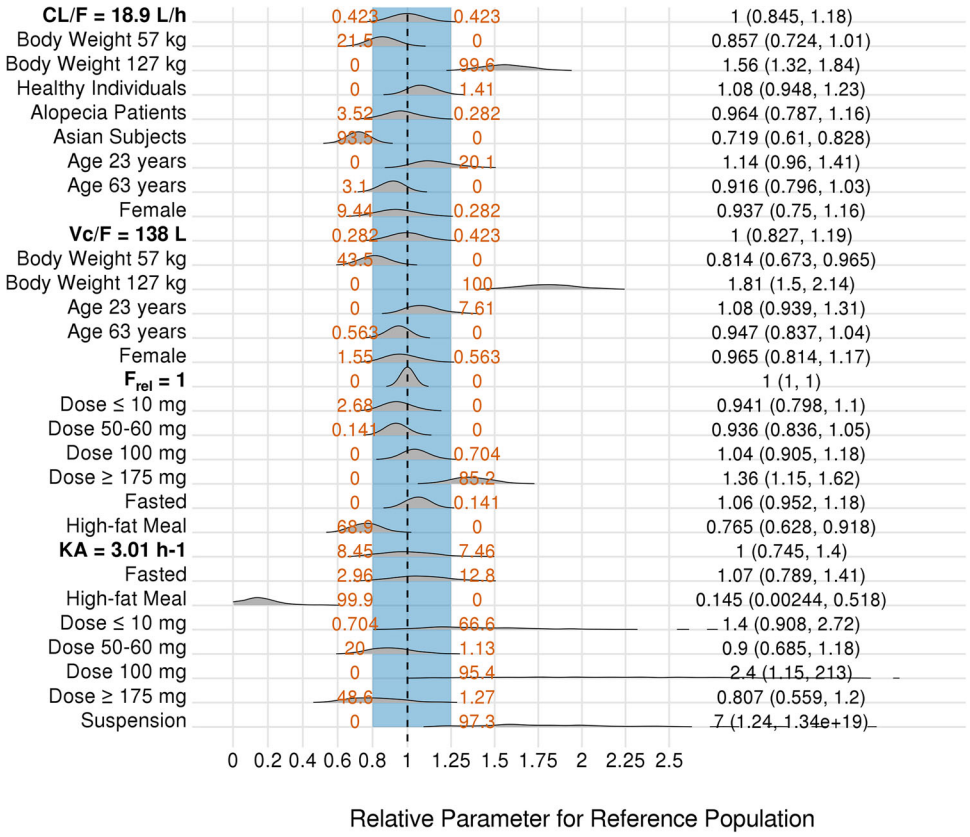

Figure 1. Full model estimation bootstrap results. The gray density distributions represent the parameter ratios across all bootstraps, red numbers are the proportion of bootstraps with ratios <0.8 (left) or >1.25 (right). Black numbers on the right *y*-axis are the median (5th and 95th percentiles) of ratios for the covariate estimate. The blue shaded region is the range of ratios from 0.8 to 1.25, and the black vertical dashed line is a ratio of 1. Allometric scaling on body weight was fixed to literature values.[9] The reference populations for CL/F, Vc/F, F_{rel}, and k_a were 70-kg White male patients with psoriasis aged 42 years taking 30 mg of brepocitinib once daily, 70-kg male participants aged 42 years, 70-kg patients with psoriasis taking 30 mg of brepocitinib without respect to food, and 70-kg patients taking 30-mg tablets of brepocitinib without respect to food, respectively. CL/F, apparent clearance; F_{rel}, relative bioavailability; k_a, absorption rate constant; Vc/F, apparent central volume.

statistically different parameter value when comparing the 2 BLQ handling methods.

The model was assessed using a VPC stratified by dose and prediction-corrected VPC provided in the Supplemental Information. The final model predictions overlay the observed data adequately, despite some overprediction of the median and variability of the maximum concentration at higher doses and underprediction of the lower confidence interval 24 hours after dosing. Steady-state concentration-time profiles showing the variability in brepocitinib predictions are shown in Figure 2. Diagnostic plots and NONMEM code for the final model are available in the Supplemental Information.

$$A_{lag,i} = 0.24 \cdot (1 - 1 \cdot Suspension) \quad (6)$$

$$k_{a,i} = 3.46 \cdot (1 - 0.699 \cdot Fed) \quad (7)$$

$$F_{rel,i} = 1 \cdot (1 - 0.283 \cdot Fed) \cdot \left(1 + 0.351 \cdot Dose_{\geq 175mg}\right) \quad (8)$$

$$CL/F_{rel,i} = 18.7 \cdot \left(\frac{BWT}{70}\right)^{0.75} \cdot (1 - 0.243 \cdot Asian) \cdot e^{\eta_{CL/F,i}} \quad (9)$$

$$Vc/F_{rel,i} = 136 \cdot \left(\frac{BWT}{70}\right) \cdot e^{\eta_{Vc/F,i}} \quad (10)$$

where $A_{lag,i}$, $k_{a,i}$, and so on are the parameter values for the *i*th individual, CL/F_{rel} and Vc/F_{rel} represent the CL/F and Vc/F before correction by relative bioavailability, *Suspension*, *Fed*, *Dose*, and *Asian* are a value of

Table 3. Parameter Estimates for Final Model

Parameter	Value (95%CI)	Bootstrap Median (95%CI)	Shrinkage (%)
Population parameter			
First-order absorption rate constant (k_a; h)	3.46 (3.04 to 3.88)	3.51 (3.13 to 4.10)	…
Apparent clearance (CL/F; L/h)	18.7 (16.9 to 20.5)	18.7 (17.1 to 20.6)	…
Apparent volume of distribution (Vc/F; L)	136 (124 to 148)	136 (125 to 148)	…
Absorption lag (A_{lag}; h)	0.240 (0.234 to 0.246)	0.240 (0.228 to 0.273)	…
Effect of weight on CL/F (70 kg reference)	0.750 (fixed)	0.750 (fixed)	…
Effect of weight on Vc/F (70 kg reference)	1.00 (fixed)	1.00 (fixed)	…
Effect of suspension formulation on A_{lag}	–1.00 (fixed)	–1.00 (fixed)	…
Effect of high-fat meal on k_a	–0.699 (–0.899 to –0.499)	–0.701 (–0.831 to –0.329)	…
Effect of dose on F_{rel} (dose $\geq$175 mg)	0.351 (0.194 to 0.508)	0.348 (0.186 to 0.508)	…
Effect of Asian subjects on CL/F	–0.243 (–0.363 to –0.123)	–0.235 (–0.346 to –0.113)	…
Effect of high-fat meal on F_{rel}	–0.283 (–0.389 to –0.177)	–0.279 (–0.391 to –0.169)	…
Interindividual variability			
$\omega_{CL/F}$ (% CV)	78.0 (57.5 to 98.5)	76.9 (68.1 to 89.4)	5.17
$\omega_{Vc/F}$ (%CV)	60.5 (27.3 to 93.5)	59.5 (45.3 to 79.0)	12.1
Correlation			
$\rho_{CL/F\text{-}Vc/F}$	0.760 (0.403 to 1.12)	0.759 (0.651 to 0.840)	…
Random unexplained variability			
Proportional RUV (phase 1; CV)	0.527 (0.444 to 0.610)	0.517 (0.441 to 0.605)	…
Proportional RUV (phase 2; CV)	0.875 (0.812 to 0.938)	0.873 (0.813 to 0.937)	…
ε_{res}	1.00 (fixed)	1.00 (fixed)	6.08

A_{lag}, absorption lag time; CL/F, apparent clearance; CV, coefficient of variation; F, absolute bioavailability; F_{rel}, relative bioavailability; k_a, absorption rate constant; RUV, random unexplained variability; SD, standard deviation; Vc/F, apparent central volume of distribution.

0 or 1 representing whether an individual meets the criteria for that categorical covariate and BWT represents the body weight of an individual, and $\eta_{P,i}$ is an independent random variable describing the variability in a given parameter, P, among subjects with a mean of 0 and variance, $\omega_P{}^2$.

Discussion

A comprehensive population PK model for oral brepocitinib was developed using pooled data from phase 1 and phase 2 studies consisting of both healthy and patient populations. Brepocitinib exposure after oral administration was adequately characterized by a 1-compartment population PK model with first-order absorption and first-order elimination with an increase in oral bioavailability when dose increased from $\leq$100 mg to $\geq$175 mg. Covariates that may affect brepocitinib PK were explored as data permitted, which included demographic factors such as weight and race, different patient populations as well as food and formulation effects.

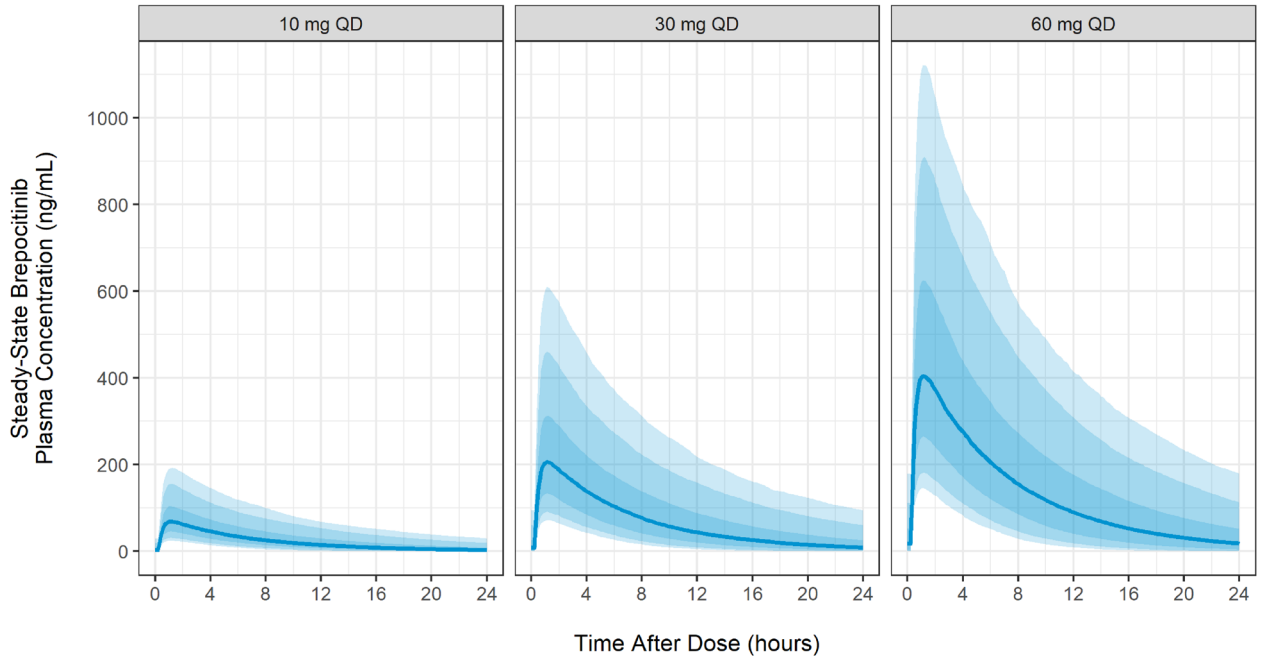

Figure 2. Steady-state concentration profiles of brepocitinib doses of interest. The median of individual predicted brepocitinib concentrations is represented by the blue lines. Percentiles of the individual predicted brepocitinib concentrations are represented by the blue shaded ribbons (darkest to lightest ribbon: 25th and 75th percentiles, 10th and 90th percentiles, 5th and 95th percentiles). Summary data were based on steady-state simulations of 2000 individuals using covariate values according to the reference population of a 70-kg White participant taking 10, 30, or 60 mg brepocitinib tablets without respect to food every day (once daily).

The nonlinear pharmacokinetics found by the noncompartmental analysis of the first-in-human pharmacokinetics of brepocitinib[6] were quantified in the present model, with patients taking doses of ≥175 mg experiencing a 35.1% higher relative bioavailability. Based on the Human Mass Balance study (NCT03770039), the fraction absorbed and absolute bioavailability after administration of 60 mg of brepocitinib was estimated to be 100% and 75%, respectively (data not shown). These data suggest that first-pass metabolism may account for the observed bioavailability. Given the absolute bioavailability of brepocitinib, the estimated dose effect on relative bioavailability is likely the maximum effect with the effect gradually increasing as doses increase from 100 to 175 mg. To fully describe the continuous dose effect on PK would require data from subjects receiving doses between 100 and 175 mg, which were not available for the present analysis. Despite this nonlinearity not being fully understood (although it is likely related to saturation of first-pass metabolism as fraction absorbed is essentially complete), it is unlikely to be clinically relevant, given that phase 2 studies have not exceeded 60-mg daily dosing.

The covariate analysis found no effects of patient population on CL/F, with the full model estimation results (Figure 1) showing no statistically or clinically significant difference between healthy participants and patient populations with plaque psoriasis or alopecia areata. Further covariate analysis will be conducted to determine whether PK parameters differ in other patient populations of interest when data become available.

The higher exposure seen in Asian populations was characterized as by a 24.3% reduction in CL/F. This effect was identified to be in addition to the reduction of CL/F already present in these patients due to this subpopulation's lower average body weight (78.5 kg vs. 87.4 kg). As brepocitinib is hepatically metabolized by CYP3A4/5 (fm = 0.77) and CYP1A2 (fm = 0.14) it is unclear why this difference in exposure is observed, given that genetic polymorphisms in these CYP enzymes are not considered primary factors in PK variability. It is acknowledged that this covariate is based on a limited number of Asian subjects with dense sampling (approximately 8% of total subjects) and there were insufficient data to characterize covariate effects in other race populations. As more data in different race populations becomes available, additional covariate effects on CL/F and possibly other PK parameters may be estimated providing a better description of the impact of race on brepocitinib PK.

Despite 10.8% of plasma observations being missing, no BLQ handling methods[11] were used due to no distinction between BLQ values and other missing values. Given the simple model structure and the fact that

any potential nonlinearity was observed at concentrations far above the limit of quantification, it is unlikely that considerable bias was introduced to parameter estimates based on this decision.[12] This decision was supported by a sensitivity analysis using the M3 method performed with the final model. The lack of significant changes in parameters is likely a result of many missing values being sampled immediately before or after dosing, where values are not expected to be evaluable given brepocitinib's half-life.

The administration of brepocitinib with a high-fat meal was found to affect absorption, with high-fat meals being associated with a 69.9% slower absorption rate and 28.3% reduction in relative bioavailability. Although the estimated reduction in relative bioavailability by high-fat meal appeared slightly greater than that determined by noncompartmental analysis (≈18%), considering the model uncertainty of this covariate effect the difference in estimates is not significant (95% CI, 16.9%–39.1%) and continues to support administration of brepocitinib without regards to food.

The suspension formulation used in the first-in-human study was best described without an absorption lag and appeared to have a faster absorption than tablet formulations during covariate analysis, despite having a longer time to maximum concentration when calculated by noncompartmental analysis. This is likely due to the inclusion of phase 2 study data in the present analysis where there were no controls for meals around dosing times. This is expected to make the typical oral absorption slower, as it represents administration for both fasted subjects and subjects who had taken a standard meal. No significant covariate effect could be estimated to differentiate fasted patients and patients administered brepocitinib without regard for food (Figure 1).

The clinical development of brepocitinib is still in progress, and as more data are collected from larger and more diversified populations, the covariates described in this analysis may be further refined and other intrinsic and extrinsic covariates will be investigated as appropriate. In summary, this initial population model adequately describes brepocitinib oral PK in healthy participants and several patient populations showing no difference between patient populations. Furthermore, it provides the framework for estimation of individual exposures for clinical trial designs with sparse PK sampling and will help relate exposures to efficacy and safety outcomes in phase 2/3 studies. The population PK model will be used to further evaluate brepocitinib PK and will provide a quantitative rationale for any future dosing decisions.

Funding

These studies were sponsored by Pfizer.

Conflicts of Interest

All authors are full-time employees of Pfizer.

Acknowledgments

Upon request, and subject to review, Pfizer will provide the data that support the findings of this study. Subject to certain criteria, conditions and exceptions, Pfizer may also provide access to the related individual deidentified participant data. See https://www.pfizer.com/science/clinical-trials/trial-data-and-results for more information.

References

1. Fensome A, Ambler CM, Arnold E, et al. Dual inhibition of TYK2 and JAK1 for the treatment of autoimmune diseases: discovery of ((S)-2,2-difluorocyclopropyl)((1R,5S)-3-(2-((1-methyl-1H-pyrazol-4-yl)amino)pyrimidin-4-yl)-3,8-diazabicyclo[3.2.1]octan-8-yl)methanone (PF-06700841). *Journal of Medicinal Chemistry*. 2018;61(19):8597-8612.
2. Nogueira M, Puig L, Torres T. JAK inhibitors for treatment of psoriasis: focus on selective TYK2 inhibitors. *Drugs*. 2020;80(4):341-352.
3. O'Sullivan LA, Liongue C, Lewis RS, Stephenson SEM, Ward AC. Cytokine receptor signaling through the Jak–Stat–Socs pathway in disease. *Molecular Immunology*. 2007;44(10):2497-2506.
4. Neurath MF. Cytokines in inflammatory bowel disease. *Nature Reviews Immunology*. 2014;14(5):329-342.
5. Guttman-Yassky E, Ungar B, Noda S, et al. Extensive alopecia areata is reversed by IL-12/IL-23p40 cytokine antagonism. *Journal of Allergy and Clinical Immunology*. 2016;137(1):301-304.
6. Banfield C, Scaramozza M, Zhang W, et al. The safety, tolerability, pharmacokinetics, and pharmacodynamics of a TYK2/JAK1 inhibitor (PF-06700841) in healthy subjects and patients with plaque psoriasis. *Journal of Clinical Pharmacology*. 2018;58(4):434-447.
7. Forman SB, Pariser DM, Poulin Y, et al. TYK2/JAK1 inhibitor PF-06700841 in patients with plaque psoriasis: phase iia, randomized, double-blind, placebo-controlled trial. *Journal of Investigative Dermatology*. 2020;140(12):2359-2370.
8. King B, Guttman-Yassky E, Peeva E, et al. A phase 2a randomized, placebo-controlled study to evaluate the efficacy and safety of the oral Janus kinase inhibitors ritlecitinib and brepocitinib in alopecia areata: 24-week

results. *Journal of the American Academy of Dermatology*. 2021;85(2):379-387.
9. Page KM, Suarez-Farinas M, Suprun M, et al. Molecular and cellular responses to the TYK2/JAK1 inhibitor PF-06700841 reveal reduction of skin inflammation in plaque psoriasis. *Journal of Investigative Dermatology*. 2020;140(8):1546-1555.
10. EFPIA MID Workgroup, Marshall SF, Burghaus R, et al. Good practices in model-informed drug discovery and development: practice, application, and documentation. *CPT Pharmacometrics and Systems Pharmacology*. 2016;5(3):93-122.
11. Beal SL. Ways to fit a PK model with some data below the quantification limit. *Journal of Pharmacokinetics and Pharmacodynamics*. 2001;28(5):481-504.
12. Irby DJ, Ibrahim ME, Dauki AM, et al. Approaches to handling missing or "problematic" pharmacology data: pharmacokinetics. *CPT Pharmacometrics and System Pharmacology*. 2021;10(4):291-308.
13. Holford NH. A size standard for pharmacokinetics. *Clinical Pharmacokinetics*. 1996;30(5):329-332.
14. Mould DR, Upton RN. Basic concepts in population modeling, simulation, and model-based drug development-part 2: introduction to pharmacokinetic modeling methods. *CPT Pharmacometrics and System Pharmacology*. 2013;2(4):e38
15. Harrell FE, Jr., Lee KL, Mark DB. Multivariable prognostic models: issues in developing models, evaluating assumptions and adequacy, and measuring and reducing errors. *Statistics in Medicine*. 1996;15(4):361-87.
16. Harrell FE. *Multivariable Modeling Strategies. Regression Modeling Strategies: With Applications to Linear Models, Logistic and Ordinal Regression, and Survival Analysis*. Springer International Publishing; 2015:63-102.
17. Gastonguay MR. A full model estimation approach for covariate effects: inference based on clinical importance and estimation precision. presented at: American Association of Pharmaceutical Scientists Annual Meeting; 2004; Baltimore, MD.
18. Agoram B, Heatherington AC, Gastonguay MR. Development and evaluation of a population pharmacokinetic-pharmacodynamic model of darbepoetin alfa in patients with nonmyeloid malignancies undergoing multicycle chemotherapy. *The AAPS Journal*. 2006;8(3):E552-E563.
19. Gastonguay MR. Full covariate models as an alternative to methods relying on statistical significance for inferences about covariate effects: a review of methodology and 42 case studies. presented at: Population Approach Group Europe Meeting; 2011; Athens, Greece.
20. Xu XS, Yuan M, Zhu H, et al. Full covariate modelling approach in population pharmacokinetics: understanding the underlying hypothesis tests and implications of multiplicity. *British Journal of Clinical Pharmacology*. 2018;84(7):1525-1534.
21. Holford N. The visual predictive check - superiority to standard diagnostic (Rorschach) plots. presented at: Population Approach Group Europe Meeting; 2005; Pamplona, Spain.
22. Karlsson MO, Savic RM. Diagnosing model diagnostics. *Clinical Pharmacology & Therapeutics*. 2007;82(1):17-20.
23. Karlsson MO, Holford N. A tutorial on visual predictive checks. presented at: Population Approach Group Europe Meeting; 2008; Marseille, France.
24. Bergstrand M, Hooker AC, Wallin JE, Karlsson MO. Prediction-corrected visual predictive checks for diagnosing nonlinear mixed-effects models. *The AAPS Journal*. 2011;13(2):143-51.
25. Beal SL, Sheiner LB, Boeckmann A, Bauer RJ. NONMEM User's Guides (1989-2009). *Icon Development Solutions*; 2009.
26. R: A language and environment for statistical computing. Version 3.5.1. R Foundation for Statistical Computing; 2018. https://www.R-project.org/
27. Lindbom L, Pihlgren P, Jonsson EN. PsN-Toolkit–a collection of computer intensive statistical methods for non-linear mixed effect modeling using NONMEM. *Computer Methods and Programs in Biomedicine*. 2005;79(3):241-57.
28. Thai H-T, Mentré F, Holford NHG, Veyrat-Follet C, Comets E. Evaluation of bootstrap methods for estimating uncertainty of parameters in nonlinear mixed-effects models: a simulation study in population pharmacokinetics. *Journal of Pharmacokinetics and Pharmacodynamics*. 2014;41(1):15-33.
29. Akaike H. A new look at the statistical model identification. *IEEE Transactions on Automatic Control*. 1974;19(6):716-723.
30. Bonate PL. The effect of collinearity on parameter estimates in nonlinear mixed effect models. *Pharmaceutical Research*. 1999;16(5):709-717.
31. Mould DR, Upton RN. Basic concepts in population modeling, simulation, and model-based drug development. *CPT Pharmacometrics and System Pharmacology*. 2012;1(9):e6.
32. Hooker AC, Staatz CE, Karlsson MO. Conditional Weighted Residuals (CWRES): a model diagnostic for the FOCE method. *Pharmaceutical Research*. 2007;24(12):2187-2197.

Supplemental Information

Additional supplemental information can be found by clicking the Supplements link in the PDF toolbar or the Supplemental Information section at the end of web-based version of this article.